PROCEEDINGS OF SCIENCE

Unveiling the Accretion Geometry of QS Tel Through Photometric, Spectroscopic, and Polarimetric Observations

L. Booi,[1,2,*] **S. B. Potter,**[2,3] **Z. N. Khangale**[1] **and P. A. Woudt**[1]

[1]*Department of Astronomy, University of Cape Town, Private Bag X3, Rondebosch 7701, South Africa*
[2]*South African Astronomical Observatory, PO Box 9, Observatory 7935, Cape Town, South Africa*
[3]*Department of Physics, University of Johannesburg, PO Box 524, Auckland Park 2006, South Africa*

E-mail: luthob847@gmail.com

We present phase-resolved photometry, spectroscopy, photopolarimetry, and circular spectropolarimetry analysis of the polar QS Tel using the observations obtained between 2017 and 2025. We report the first detection of quasi-periodic oscillations (QPOs) in QS Tel, with timescales of 2–8 minutes and 8–11 minutes, revealing dynamic accretion behaviour. Doppler maps of the Hα and He II λ4686 emission lines, reveal three components of the system which are the irradiated face of the secondary star, the ballistic stream and the magnetically confined accretion stream. In the flux modulated maps, the magnetically confined accretion stream splits into two distinct components, we associate the two components to two distinct magnetically confined accretion streams. We report circular polarization which varies between -10% to $+25\%$. In addition, we identified two broad cyclotron harmonics centred at λ4800 and λ6300. From the spacing between the harmonics, we determine a magnetic field strength of 53 MG and harmonic numbers 4 and 3, respectively.

High Energy Astrophysics in Southern Africa (HEASA2025)
16-20 September, 2025
University of Johannesburg, South Africa

*Speaker

 ISSN 1824-8039 . Published by SISSA Medialab.

PoS(HEASA2025)048

1. Introduction

Cataclysmic variables (CVs) are semi-detached binary systems in which a white dwarf (WD) accretes material from a Roche-lobe–filling companion star [1, 2]. CVs are generally divided into two main groups: non-magnetic and magnetic cataclysmic variables (mCVs). The accretion mode in mCVs depends primarily on the magnetic field strength of the WD. When the magnetic field strength is approximately 1–10 MG [1, 3], a partial accretion disc can form, as the field is too weak to completely disrupt the disc but strong enough to truncate its inner regions; such systems are referred to as intermediate polars [1, 3]. In polars, where the magnetic field strength ranges from about 10–80 MG [1–3], the strong magnetic field prevents disc formation entirely. Instead, the accreted material follows a ballistic trajectory before coupling to the magnetic field lines and being channelled onto the magnetic poles. At field strengths 80 MG < B < 230 MG [1, 2, 4], the material couples directly to the magnetic field lines without forming a ballistic stream, accreting almost immediately onto the poles [1–3]. A defining characteristic of CVs is continuous mass transfer from the secondary star to the WD, and variations in the mass transfer result in variability detectable in light curves. Variability occurs over a wide range of timescales and are generally classified as intrinsic or extrinsic. Short-timescale variations (seconds to days) include intrinsic phenomena such as flickering and quasi-periodic oscillations (QPOs). In polars, QPOs are attributed to oscillations of the radiative accretion shock formed where the accretion flow impacts the magnetic poles [5]. QS Tel (= RXJ 1938.6-4612) is a polar which was first identified in ROSAT PSPC survey data by Buckley et al. [6] and later confirmed as the brightest polar. Optical photometry and spectroscopy established its classification as a polar with an orbital period of 2.33 h [6–8], placing it within the 2–3 h period gap where magnetic braking weakens as the secondary star becomes fully convective [9]. QS Tel exhibits a complex, variable accretion geometry: optical and EUV light curves, circular polarization up to 5%, and radial velocity variations indicate two-pole accretion, with the secondary pole dominating EUV/X-ray emission and the primary contributing mainly to optical flux [8, 9]. During a low accretion state, spectropolarimetry revealed one-pole accretion with B ∼ 56 MG at the active pole [10]. In a subsequent high state, the second pole became active again, and B ∼ 47 MG and B ∼ 70–80 MG for the two poles indicated a non-dipolar field structure [7]. In this paper, we present multi-wavelength observations of QS Tel in order to investigate its long-term variability, accretion behaviour and polarization characteristics.

2. Results

2.1 Photometry

Phase-resolved photometric observations were obtained on 5 and 21 July 2024 using the SAAO 1-m telescope with the Sutherland High-speed Optical Camera (SHOC; [11]) in clear filter mode mounted on the telescope. Data reduction was performed using the IO_Phot software[1], developed by Dr Stephen Potter, which is specifically designed to process SHOC data cubes. Figure 1

[1] IO_Phot is a Python-based pipeline for aperture photometry, developed at SAAO, and available at https://www.saao.ac.za/~sbp/IO_phot/IO_phot.py

presents the SHOC photometric light curve (top panel) and the corresponding trailed Lomb–Scargle periodogram (bottom panel). The light curve exhibits short-term, irregular brightness fluctuations caused by instabilities in the accretion flow onto the magnetic WD, which are characteristic of quasi-periodic oscillations (QPOs) [5]. The trailed power spectrum reveals transient QPO features that evolve in both amplitude and frequency throughout the observation, indicating a non-stationary origin. The QPOs occur on timescales of approximately 2–8 minutes and 8–11 minutes, consistent with oscillations arising from inhomogeneous accretion or magnetically confined shocks near the accretion region [12]. These rapid variations suggest dynamic changes in the accretion column structure during the high accretion state of this system [13, 14].

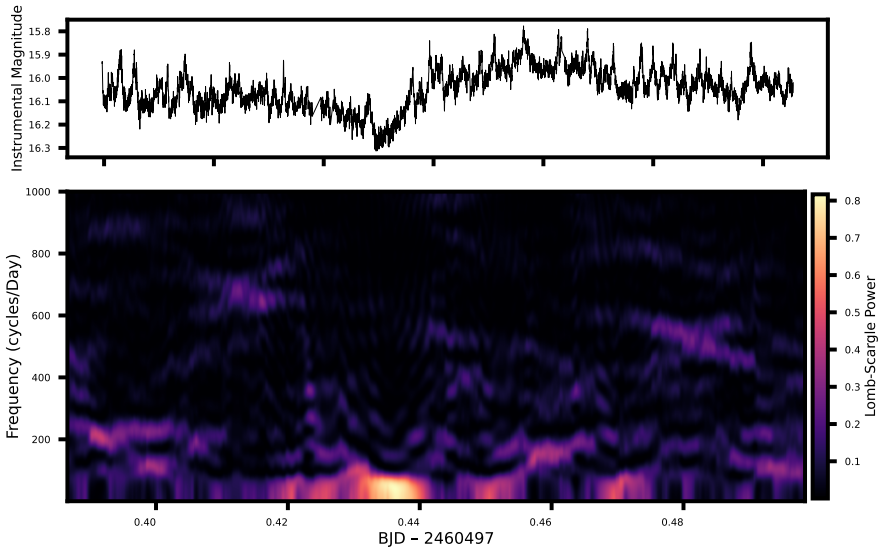

Figure 1: The light curve (top) and trailed Lomb-Scargle periodogram (bottom) of QS Tel from the observations obtained on 5 July 2024. The color scale represents the normalized Lomb-Scargle power, highlighting the presence and evolution of quasi-periodic oscillations (QPOs) during the night.

2.2 Spectroscopy

Phase-resolved spectroscopic observations of QS Tel were obtained with the SAAO 1.9-m telescope using the Spectrograph Upgrade – Newly Improved Cassegrain (SpUpNIC; [15]) spectrograph, with 250-s exposures covering $\lambda\lambda$4050–5250 in grating 4 on 21 September 2022 and $\lambda\lambda$6250–7250 in grating 5 on 23 September 2022. Arc lamp exposures (CuAr for grating 4 and CuNe for grating 5) were taken at frequent intervals after 8 exposures for wavelength calibration purposes. A slit width of 1.5 arcsec was used. Data reduction was performed using standard procedures in `IRAF`[2][16]. The upper panel of Figure 2 shows the bluer part of the spectrum, while the lower panel shows the redder wavelengths. The spectra exhibit typical features of an mCV in a high state, with strong hydrogen Balmer (e.g. Hβ, Hγ) and single-ionised helium emission lines, along with a weak Bowen blend and carbon emission. The red spectrum shows prominent Hα emission, together with He I λ6678. The narrow absorption feature at λ6867 is a telluric sky line.

[2] `IRAF` (Image Reduction and Analysis Facility) is a software suite for the reduction and analysis of astronomical data.

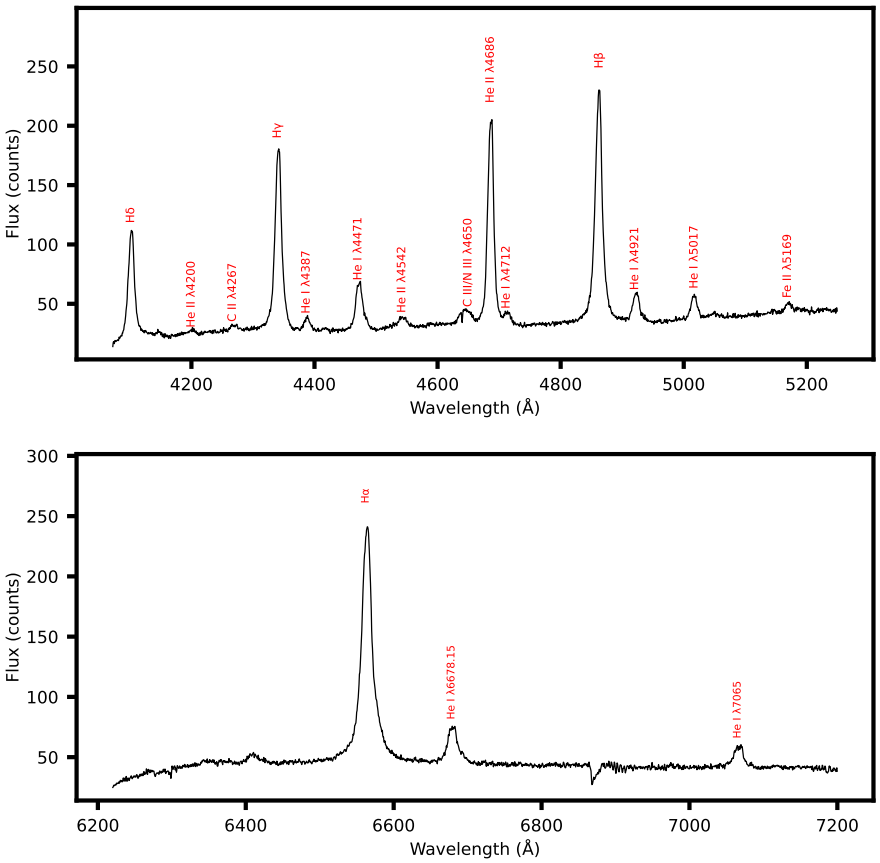

Figure 2: Average spectra of QS Tel obtained using the SAAO 1.9-m/SpUpNIC. Top panel: The bluer spectrum obtained on 21 Sep 2022 with Grating 4. Bottom Panel: The redder spectrum obtained on 23 Sep 2022 with Grating 5. The observed absorption line at λ6867, is a telluric sky line.

2.2.1 Flux Modulated maps

Doppler tomography is an indirect imaging technique used to map the velocity structure of emitting material in interacting binary systems [17]. It reconstructs two-dimensional velocity maps from time-resolved spectra obtained over the orbital cycle, allowing us to identify the regions where the emission lines originated. The standard (left panels) and inside-out (right panels) flux modulated maps of HeII λ4686 and Hα shown in Figures 3 and 4, reveal emission from the irradiated face of the secondary star, the ballistic stream, and the magnetically confined accretion stream. Notably, the magnetically confined stream appears to split into two components in the lower-left quadrant of the maps. We associate the two components with two magnetically confined accretion streams. The phase-of-maximum-flux maps seen in the middle panels of Figures 3 and 4 show orbital phase at which each emission component appears brightest to the observer. Only pixels with modulation amplitudes exceeding 10% of the maximum are shown. The color-coding follows orbital phase: 0.0 (black), 0.25 (red), 0.5 (green), and 0.75 (blue). The secondary star is mostly flux modulated at phase 0.5, which appears as a green region within the Roche lobe of the secondary star. This is consistent with expectations, as the irradiated face of the secondary star points toward the observer

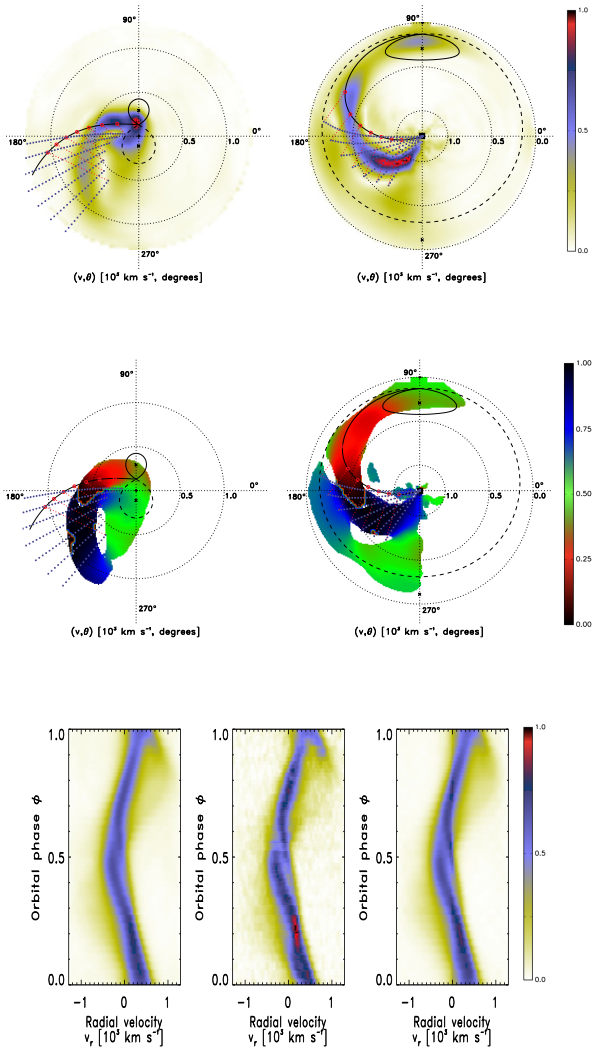

Figure 3: Standard and inside-out Doppler maps and trailed observed and reconstructed spectra based on the HeII λ4686 emission line. Top row: the standard and inside-out modulation amplitude Doppler maps. Middle row: the standard and inside-out phase of maximum flux Doppler maps. Bottom row: the input trailed spectra (centre) with the summed reconstructed trailed spectra for the ten consecutive half-phases for standard (left) and inside-out (right), respectively.

at this phase. The ballistic stream, shown in red on the maps, is primarily modulated around orbital phase 0.25. At this phase, the observer has a full view of the ballistic stream, particularly the portion closest to the accreting WD, where the emission is strongest. The magnetically confined accretion stream, in contrast, appears in the lower-left region of the maps as a mixture of blue, black, and green, reflecting its more complex velocity structure and modulation.

2.3 Circular Spectropolarimetry

Circular spectropolarimetric observations were acquired with the South African Large Telescope (SALT; [18]) using the Robert Stobie Spectrograph (RSS; [19]) in circular spectropolarimetry mode

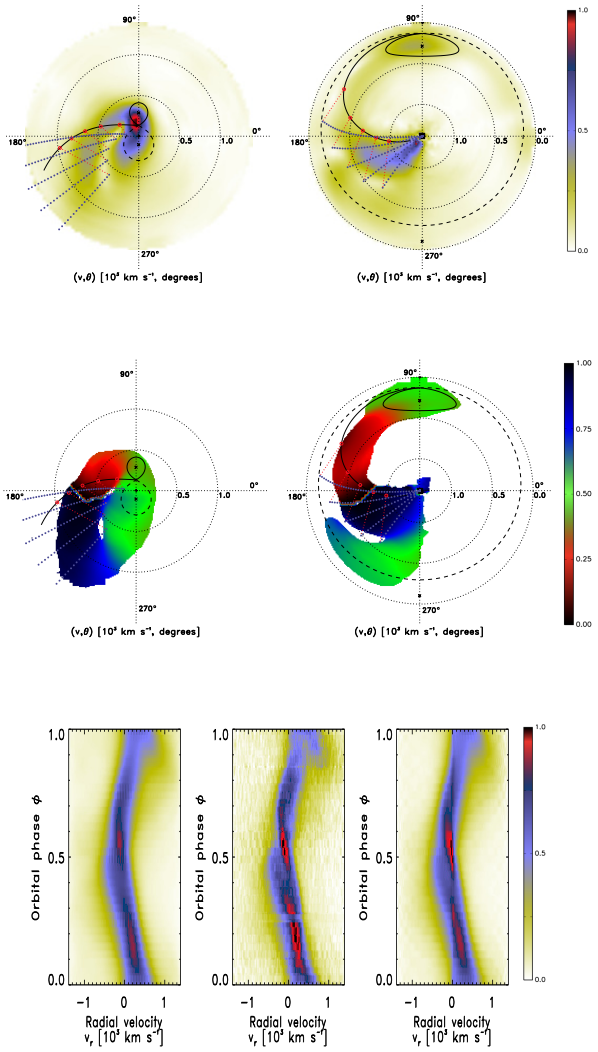

Figure 4: Standard and inside-out Doppler maps and trailed observed and reconstructed spectra based on the Hα emission line. Top row: the standard and inside-out modulation amplitude Doppler maps. Middle row: the standard and inside-out phase of maximum flux Doppler maps. Bottom row: the input trailed spectra (centre) with the summed reconstructed trailed spectra for the ten consecutive half-phases for standard (left) and inside-out (right), respectively.

[20] over multiple epochs between May 2023 and August 2025. The exposure time of 300 s was used. PG0900 grating was used with a grating angle of 14.75° giving a wavelength range coverage of $\lambda\lambda$4060–7250. The data were reduced with the POLSALT-BETA[3] pipeline, which is based on the PYSALT package. Figure 5 shows the circular spectropolarimetry results of QS Tel, showing instrumental flux (left column), the circular polarization percentage (middle column) and the total polarized flux (right column). The degree of circular polarization varies between –10% and +25% over the orbital cycle. We identified two broad phase-dependent cyclotron humps centred at λ4800 and λ6300 detectable at phase 0.343. From the spacing of the harmonics we inferred a magnetic

[3]For more details, see https://github.com/saltastro/polsalt/

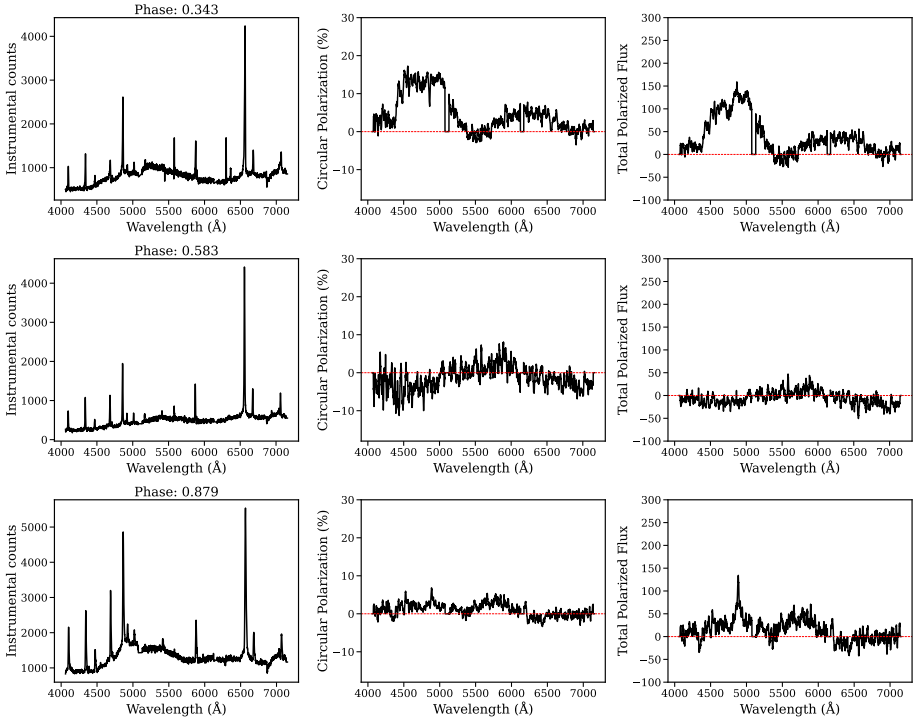

Figure 5: Spectropolarimetric data of QS Tel obtained during the intermediate accretion state between May 2023 and August 2025, folded over the orbital phase. The left column shows the instrumental flux, the middle column displays the circular polarization percentage, and the right panel presents the total polarised flux.

field strength of 53 MG. These features are associated with harmonic numbers 4 and 3, consistent with the previous studies [7].

3. Discussion and Conclusions

We present photometry, spectroscopy, and circular spectropolarimetry of QS Tel obtained during intermediate and high accretion state. The SHOC light curves show a gradual brightening and the presence of QPOs on timescales of 2–8 and 8–11 minutes, indicating short-term variability associated with instabilities in the accretion flow. The optical spectra are dominated by strong Balmer and HeII $\lambda\lambda$4686 emission, consistent with QS Tel being in a high accretion state. The Doppler maps reveal emission from the irradiated face of the secondary star, as well as from both the ballistic stream and the magnetically confined accretion stream. The magnetically confined accretion stream seen in the lower-left region of the maps splits into two components. We associate this with two magnetically confined accretion streams, a phenomenon rarely resolved in polars; recent studies of EF Eri show similar results [21], possibly supporting a two-pole accretion geometry in which both magnetic poles are actively accreting material. Circular spectropolarimetry shows polarization varying between −10% and +25%, with two broad phase-dependent cyclotron humps centred at approximately λ4800 and λ6300. From the spacing of the cyclotron harmonics, we estimate a magnetic field strength of about 53 MG, consistent with previous studies [7, 10].

4. Acknowledgements

The spectroscopic and ground based photometric observations taken using the South African Astronomical Observatory (SAAO) facilities, the SAAO 1.0-m and 1.9-m telescopes. Spectropolarimetry observations were taken using the Southern African Large Telescope (SALT) under programs 2023-1-SCI-027, 2024-1-SCI-011, and 2025-1-SCI-016 (PI: Z. N. Khangale). This work was financially supported by the National Astrophysics and Space Science Programme (NASSP).

References

[1] Warner, B. 1995, *Cataclysmic Variable Stars*, Cambridge Astrophysics Series, Vol. 28 (Cambridge: Cambridge Univ. Press)

[2] Hellier, C. 2001, *Cataclysmic Variable Stars* (Springer)

[3] Cropper, M. 1990, Space Science Reviews, 54, 195

[4] Ferrario, L., Wickramasinghe, D. T., Bailey, J., et al. 2003, MNRAS, 338, 340

[5] Breytenbach, H., Buckley, D. A. H., Bonnet-Bidaud, J. M., & Mouchet, M. 2015, in *The Golden Age of Cataclysmic Variables and Related Objects – III (Golden2015)*, 18

[6] Buckley, D. A. H., O'Donoghue, D., Hassall, B. J. M., et al. 1993, MNRAS, 262, 93

[7] Schwope, A. D., Thomas, H.-C., Beuermann, K., et al. 1995, A&A, 293, 764

[8] Rosen, S. R., Mittaz, J. P. D., Buckley, D. A. H., et al. 1996, MNRAS, 280, 1121

[9] Traulsen, I., Reinsch, K., Schwope, A. D., et al. 2011, A&A, 529, A116

[10] Ferrario, L., Wickramasinghe, D. T., Bailey, J., et al. 1994, MNRAS, 268, 128

[11] Coppejans, R., Woudt, P. A., Warner, B., et al. 2013, PASP, 125, 976

[12] Bera, R., & Bhattacharya, D. 2018, MNRAS, 474, 1629

[13] Schwope, A. D. 1990, Reviews in Modern Astronomy, 3, 44

[14] Potter, S. B., Buckley, D. A. H., O'Donoghue, D., et al. 2010, MNRAS, 402, 1161

[15] Crause , L. A., Buckley, D. A. H., Crawford, S., et al. 2019, JATIS, 5, 024007

[16] Tody, D. 1986, SPIE, 627, 733

[17] Marsh, T. R., & Horne, K. 1988, Oxford University Press

[18] Burgh, E. B., Nordsieck, K. H., Kobulnicky, H. A., et al. 2006, SPIE, 6267, 0Z

[19] Burgh, E. B., Nordsieck, K. H., Kobulnicky, H. A., et al. 2003, SPIE, 4841, 1463

[20] Nordsieck, K. H., Burgh, E. B., Kobulnicky, H. A., et al. 2003, SPIE, 4843, 170

[21] Khangale, Z. N., Potter, S. B., Buckley, D. A. H., & Barrett, P. E. 2025, MNRAS, 544, 309